

Impaired tyrosine phosphorylation of membrane type 1-matrix metalloproteinase reduces tumor cell proliferation in three-dimensional matrices and abrogates tumor growth in mice

Carine Nyalendo^{1,3}, Edith Beaulieu¹, Hervé Sartelet²,
Marisol Michaud^{1,3}, Nicolas Fontaine¹, Denis Gingras¹ and
Richard Béliveau^{1,3,*}

¹Laboratoire de Médecine Moléculaire, Centre de Cancérologie Charles-Bruneau, CHU Sainte-Justine, 3175 Chemin Côte-Ste-Catherine, Montréal, Québec, Canada H3T 1C5, ²Département de Pathologie, CHU Sainte-Justine, 3175 Chemin Côte-Ste-Catherine, Montréal, Québec, Canada H3T 1C5 and ³Centre de Recherches Biomédicales (Biomed), Université du Québec à Montréal, C.P. 8888, succursale Centre-Ville, Montréal, Québec, Canada H3C 3P8

*To whom correspondence should be addressed. Laboratoire de Médecine Moléculaire Ste-Justine-UQAM, Centre de cancérologie Charles-Bruneau, 3175, Chemin Côte-Ste-Catherine, Montréal, Québec, Canada H3T 1C5. Tel: +1 514 345 2366; Fax: +1 514 345 2359; Email: molmed@recherche-ste-justine.qc.ca

Pericellular proteolysis of the extracellular matrix by membrane type 1-matrix metalloproteinase (MT1-MMP) confers tumor cells with the ability to proliferate within three-dimensional (3D) matrices and sustains tumor growth in mice. In this study, we show that in addition to its matrix-degrading activity, phosphorylation of MT1-MMP on its unique tyrosine residue located within its cytoplasmic sequence (Tyr573) may also participate to these processes. Fibrosarcoma cells expressing a proteolytically active but non-phosphorylatable mutant of MT1-MMP showed a markedly reduced proliferation rate when embedded within 3D type I collagen matrices, this antiproliferative effect being correlated with arrest in the G₀/G₁ phase of the cell cycle. Impaired tyrosine phosphorylation of MT1-MMP also inhibits anchorage-independent growth of HT-1080 cells in soft agar as well as their invasion of collagen barriers, two prominent attributes of tumor cells, suggesting a broad inhibitory effect of the MT1-MMP mutant on tumorigenesis. Accordingly, whereas HT-1080 cells formed well-vascularized tumors containing tyrosine-phosphorylated MT1-MMP, tumor growth was completely abolished by expression of the non-phosphorylatable MT1-MMP mutant. These findings thus indicate a close co-operation between the matrix-degrading activity of MT1-MMP and tyrosine phosphorylation of its intracellular domain for tumor cell invasion and proliferation and suggest that the targeting of the intracellular signaling pathways leading to tyrosine phosphorylation of MT1-MMP may represent an unexpected alternative strategy for the inhibition of this enzyme.

Introduction

The degradation of extracellular matrix (ECM) proteins by members of the matrix metalloproteinases (MMPs) plays a crucial role in several processes underlying tumor progression, including cell attachment, cell migration, invasiveness, cell proliferation, apoptosis and angiogenesis (1–4). Recent studies have provided convincing evidence that membrane type 1-matrix metalloproteinase (MT1-MMP), a membrane-anchored MMP, plays essential roles in tumor cell migration and invasion by acting as a potent matrix-degrading protease that proteolyzes a broad spectrum of ECM proteins (5–7) as well as

Abbreviations: BB, binding buffer; cDNA, complementary DNA; 2D, two dimensional; 3D, three dimensional; ECM, extracellular matrix; FBS, fetal bovine serum; FITC, fluorescein isothiocyanate; HPS, hematoxylin, phloxin and saffron; MEM, minimum essential medium; MMP, matrix metalloproteinases; MT1-MMP, membrane type 1-matrix metalloproteinase; PBS, phosphate-buffered saline; PI, propidium iodide; TIMP, tissue inhibitor of matrix metalloproteinases.

a number of cell surface-associated adhesion receptors (8,9). MT1-MMP is overexpressed in many types of tumors (10,11) and pericellular proteolysis of the dense cross-linked meshwork of type I collagen fibrils mediated by the enzyme confers neoplastic cells with tissue-invasive activity (12) and sustains tumor cell growth in otherwise growth-restrictive three-dimensional (3D) matrices (13).

In addition to its important matrix-degrading activity, MT1-MMP contains a short cytoplasmic sequence whose function remains largely unknown but seems important. Cells expressing cytoplasmic domain-deleted MT1-MMP mutants retain the ability to proteolyse the ECM but have a markedly reduced migratory potential (14–18), suggesting a role of this domain in linking extracellular proteolysis to intracellular-signaling events involved in cell locomotion. Actually, the cytoplasmic sequence of MT1-MMP actively participates to the internalization of the enzyme (15), to the activation of the extracellular signal-Regulated Kinases-signaling pathway (17,19) as well as to its interaction with tyrosine-phosphorylated caveolin-1 (18), and these events may all contribute to efficient cell locomotion triggered by the enzyme. More recently, we reported that MT1-MMP is phosphorylated on its unique cytoplasmic tyrosine residue and that this event may also participate to cell migration (20), possibly by inducing a relocalization of the enzyme at the leading edge of migrating cells (21).

Although the mechanisms leading to the Src family kinase-dependent tyrosine phosphorylation of MT1-MMP remain to be unveiled, we observed that expression of a dominant-negative, non-phosphorylatable MT1-MMP mutant inhibits phosphorylation of the enzyme and interferes with the migration of both tumor and endothelial cells (20). We report herein that impaired tyrosine phosphorylation of MT1-MMP also markedly reduces the tumorigenic properties of the highly invasive HT-1080 fibrosarcoma cell line by interfering with the proliferation of these cells within type I collagen 3D matrices, leading to a complete inhibition of tumor growth in nude mice.

Materials and methods

Generation of cell lines

The complementary DNAs (cDNAs) encoding the full-length human MT1-MMP and its cytoplasmic domain mutant (Y573F) have been described (20). Human fibrosarcoma cells HT-1080 [grown in minimum essential medium (MEM) supplemented with 1 mM sodium pyruvate, 10% fetal bovine serum (FBS) and 4 mM glutamine] were transfected using the FuGENE 6 transfection reagent (Roche Diagnostics, Laval, QC, Canada) according to the manufacturer's instructions. Stably transfected cells were selected and maintained in 250 µg/ml Zeocin (Invitrogen, Burlington, ON, Canada). Control cells were stably transfected with the empty vector (pcDNA3.1) and were selected and maintained in 200 µg/ml G418. Stable clones expressing high levels of MT1-MMP messenger RNA and that exhibit high activity of MMP-2 activation (compared with control cells) were used. The selected stable clones were assessed for two-dimensional (2D) and 3D cell proliferation, flow cytometry and zymography assays. Data presented in this manuscript represent the results obtained from at least three independent clones.

2D–3D culture and cell invasion

Type I collagen was extracted from rat tail and resuspended at 2.7 mg/ml in acetic acid. For 2D culture, stable clones were seeded on dishes plates coated with 100 µg/ml type I collagen. For 3D culture, stable clones were mixed with 10× MEM, 0.17 N NaOH and 2.7 mg/ml type I collagen. The mixture was allowed to gel for 45 min at 37°C and culture media containing 10% FBS was added atop. For growth inhibition, 50 ng/ml of tissue inhibitor of matrix metalloproteinases-1/2 (Chemicon International, Temecula, CA) and 50 µM GM6001 (Calbiochem, San Diego, CA) were incorporated into both the collagen gel and the culture medium. Collagen gels were dissolved with 2 mg/ml bacterial collagenase (Sigma, Burlington, ON, Canada) and viable cells were counted by trypan blue exclusion using a hemacytometer. For cell invasion assays, type I collagen (0.5 mg/ml) was allowed to gel in the upper well of 24 mm Transwells

(Corning, Lowell, MA). After gelling, 5×10^5 cells in medium without serum were added atop of the collagen gel, and medium with serum (10% FBS) was added to the lower chamber. After 48 h, cells that had invaded the gel were quantified using computer-assisted imaging Northern Eclipse 6.0. The data are expressed as the average density of migrated cells per four fields. For cell invasion in dense collagen gels (2.2 mg/ml), the same procedure was applied except that cells were allowed to invade the matrix during 8 days. Collagen gels were then fixed with 10% formalin phosphate, paraffin embedded and stained with hematoxylin, phloxin and saffron (HPS).

RNA isolation and real-time quantitative polymerase chain reaction

Stable clones were cultured within type I collagen matrix (2.2 mg/ml) for 5 days. Cells were extracted with collagenase and total RNA was isolated using QIAzol lysis reagent (Qiagen, Mississauga, ON, Canada) according to the manufacturer's instructions. Equal amounts (2 µg) of purified RNA were used to synthesize first-strand cDNA with the High Capacity cDNA Reverse Transcription Kit (Applied Biosystems, Foster City, CA). Quantitative polymerase chain reaction for gene quantification was performed from first-strand cDNA using the iQTM SYBR[®] Green Supermix (Bio-Rad, Mississauga, ON, Canada) and the following primers designed for the human MT1-MMP gene: forward, 5'-GAGGGCTGCCTACCGACAAGAT-3' and reverse, 5'-CCTTCCCAGAC-TTGTATGTTCTTGG-3'. β-Actin (primers from Qiagen) was used as internal control. DNA amplification was achieved on the iQ5 Real-Time PCR Detection System (Bio-Rad) in the following conditions: 1 cycle (10 min at 95°C) then 40 cycles (10 s at 95°C; 30 s at 60°C and 30 s at 72°C) and finally 41 cycles of increasing the temperature 1°C every 10 s starting at 55°C.

Immunofluorescence and confocal microscopy

Stable clones were cultured within type I collagen matrix (2.2 mg/ml) during 5 days. Collagen gels were then fixed with 10% formalin phosphate, paraffin embedded, cut in 3 µm thick sections and mounted into pretreated slides (Superfrost +). Paraffin was removed using toluene and the samples were rehydrated with ethanol. For antigen retrieval, the samples were incubated in citrate buffer for 10 min at 95°C and cooled in the same buffer at room temperature for 20 min. After 10 min of incubation with 20 µM Hoechst for nuclei staining, samples were permeabilized with 0.2% Triton X-100 for 10 min and blocked (1% bovine serum albumin in Tris buffer saline containing 0.1% Tween 20) for 30 min. Samples were then incubated with tetramethylrhodamine B isothiocyanate-conjugated phalloidin (for actin staining) for 30 min and stained with specific primary antibodies against phospho-MT1-MMP (20) or MT1-MMP (MAB3328, Chemicon International) for 30 min, followed by 30 min incubation with Alexa488-conjugated secondary antibodies (Molecular Probes—Invitrogen, Burlington, ON, Canada). Samples were covered with Immuno-Fluore Mounting Medium (MP Biomedicals, Solon, OH). Immunostaining was visualized and photographed using a Zeiss LSM 510 Meta confocal microscope.

Anchorage-independent growth assay

Six-well plates were covered with 1.5 ml of 0.5% agar (Sigma, Oakville, ON, Canada) in complete medium (MEM, 1 mM pyruvate and 10% FBS). A total of 2×10^4 cells were suspended in 6 ml of 0.35% agar in complete medium, and 1.5 ml of this mixture (5×10^3 cells) were added atop the 0.5% agar. Cells were allowed to form colonies for 15 days at 37°C. Colonies were stained overnight with 0.005% crystal violet. Microscopic colonies were visualized and counted using light microscope (objective $\times 4$), whereas macroscopic colonies were visible to the naked eye.

Flow cytometry analysis of MT1-MMP

Cells were harvested with 0.5 mM ethylenediaminetetraacetic acid/phosphate-buffered saline (PBS) and washed twice with binding buffer (BB) containing 0.1% bovine serum albumin in PBS. In experiments using cells grown in 3D collagen matrices, cells were first extracted from the gels using bacterial collagenase and then processed for analysis. A total of 10^6 cells were incubated for 1 h at 4°C with 1 ml of 1 µg/ml MT1-MMP (MAB3328) antibody or a control mouse IgG (Sigma) in BB, washed twice with BB and incubated with anti-mouse fluorescein isothiocyanate (FITC)-conjugated antibody for 30 min at 4°C in the dark. After two washes, cells were resuspended in 1 ml BB and analyzed using the fluorescent activated cell sorting (FACS) Calibur (BD Biosciences, Mississauga, ON, Canada).

Annexin V-propidium iodide staining

Cells were harvested with 0.5 mM ethylenediaminetetraacetic acid/PBS, washed twice with PBS, double stained with FITC-Annexin V and propidium iodide (PI) using the ApoAlert[®] Annexin V Apoptosis Kit (BD Biosciences—Clontech, Oakville, ON, Canada) according to the manufacturer's instructions and analyzed using the FACS Calibur. Double staining of cells with FITC-Annexin V and PI permits the discrimination of living cells (FITC-PI-),

early apoptotic (FITC+PI-), late apoptotic (FITC+PI+) or necrotic cells (FITC-PI+).

Aneuploidy and cell cycle analysis

Cells were trypsinized, washed twice with PBS containing 5 mM ethylenediaminetetraacetic acid and fixed (10^6 cells) in 75% ethanol overnight at -20°C. In experiments using cells grown in 3D collagen matrices, cells were first extracted from the gels using bacterial collagenase prior to fixation in ethanol. Cells were then washed twice and stained with 50 µg/ml PI containing 20 µg/ml RNase A for 1 h at 37°C in the dark. Cell cycle and DNA content were then analyzed using FACS Calibur (BD Biosciences).

Immunoprecipitation and western blotting

The procedures have been described previously (18). Briefly, equal amounts of proteins were incubated overnight at 4°C in the presence of 1 µg/ml of MT1-MMP monoclonal antibody and the immune complexes were collected by incubating the mixtures with protein G-coupled Sepharose beads. Bound material was solubilized in Laemmli sample buffer, boiled for 5 min, separated by sodium dodecyl sulfate-polyacrylamide gel electrophoresis and immunoblotted.

Zymography

A total of 20 µl of conditioned media was resuspended in non-reducing sample buffer and subjected to sodium dodecyl sulfate-polyacrylamide gel electrophoresis using polyacrylamide gels containing 1 mg/ml gelatin. Gels were then washed twice for 30 min in 2.5% Triton X-100 and rinsed with nanopure water. Gels were incubated at 37°C in zymography buffer (50 mM Tris pH 7.6, 200 mM NaCl, 5 mM CaCl₂ and 0.02% Brij 35) for 18 h and digested areas were visualized by coloration of the gels with Coomassie Blue.

Measurement of collagenolytic activity

Collagenolytic activity of HT-1080 transfectants grown in 3D collagen gels was determined by the measure of hydroxyproline released in the culture media as described (22).

In vivo tumor growth

Six-week-old female immunodeficient nude mice (CrI: CD-1[®] -Foxn^{nu}) were purchased from Charles River Laboratories (Wilmington, MA). Experiments were performed according to the guidelines of the Canadian Council of Animal Care. A total of 5×10^6 viable cells (stably transfected clones) were resuspended in 100 µl of 1% methylcellulose in serum-free MEM. Mice were anesthetized with O₂/isoflurane inhalation and cells were implanted subcutaneously into the flank of mice. The tumor size was measured every 3 days using a digital caliper. Tumor size was calculated as follows: $\pi/6 \times \text{length} \times \text{width}^2$. Animals were killed after 34 days.

Histological analysis and immunohistochemistry

Tumor xenografts were fixed in 10% formalin phosphate and embedded in paraffin. For routine histological examination, 3 µm thick sections were stained with HPS. Immunohistochemistry was performed on paraffin-embedded sections using the biotin-streptavidin peroxidase LSAB kit in conjunction with an automated DAKO immunostainer (Dako, Mississauga, ON, Canada). First, for antigen retrieval, deparaffinized and rehydrated sections were incubated in citrate buffer for 30 min. The sections were then mounted in the DAKO autostainer, covered with H₂O₂ for 5 min, followed by a 5 min application of Ultra V block (Lab vision, Fremont, CA). The slides were then incubated at room temperature with anti-CD31 (PECAM-1, Santa Cruz Biotechnology, Santa Cruz, CA), anti-MT1-MMP AB815 (Chemicon International) and anti-phospho-MT1-MMP or non-specific mouse or rabbit IgG as negative controls, followed by the addition of the labeled biotin-streptavidin reagents, according to the manufacturer's instructions (LSAB + System HRP Kit; DAKO). DAB (DAKO) was used as a chromogen.

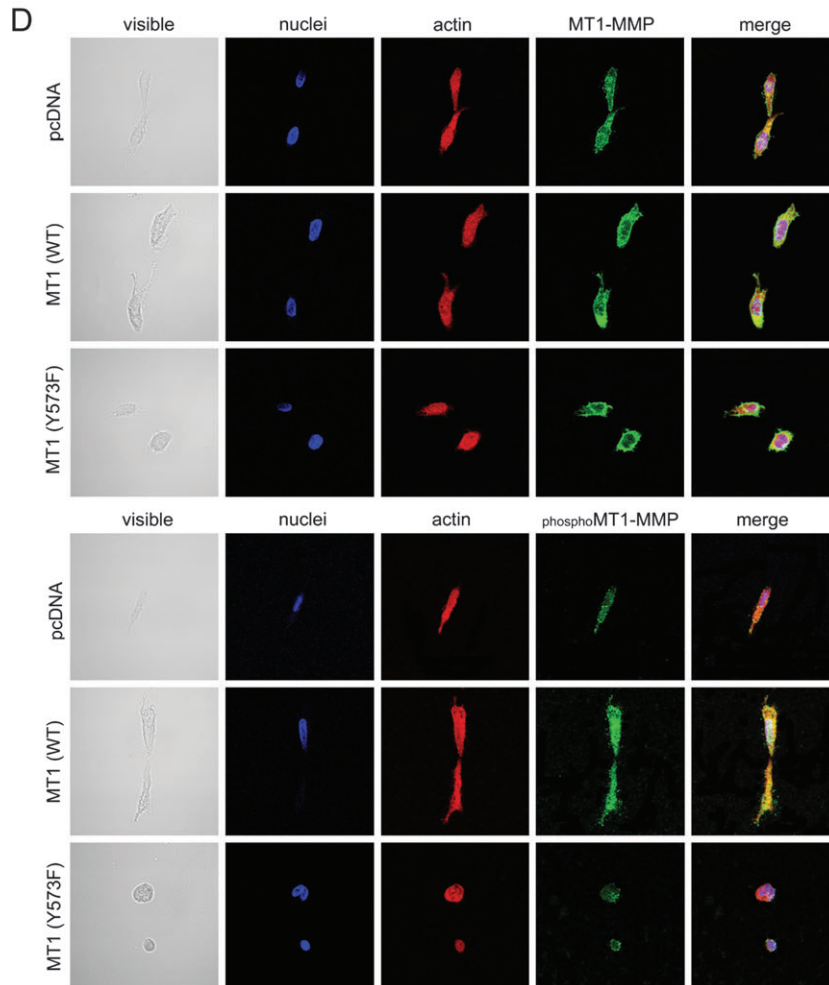
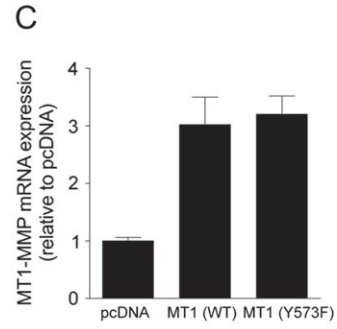
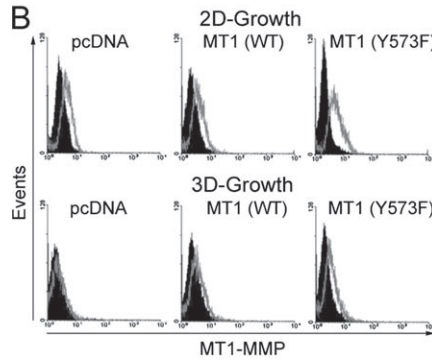
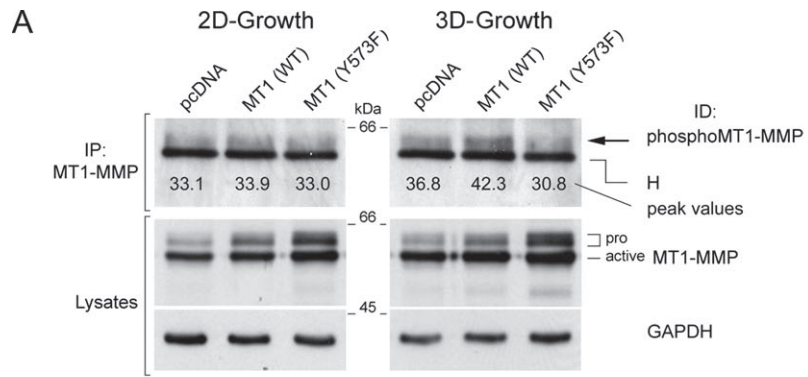
Statistical analysis

All statistical analysis was performed by one- or two-way analysis of variance followed by the Bonferroni posttests. Analyses were performed using Graph-Pad Prism program. $P < 0.05$ was considered statistically significant.

Results

A non-phosphorylatable MT1-MMP mutant reduces tumor cell proliferation within 3D matrices

We generated stable clones of human fibrosarcoma cells (HT-1080) expressing either the wild-type form of MT1-MMP (MT1 WT) or a non-phosphorylatable version of the enzyme (MT1 Y573F) (Figure 1A). Using antibodies specifically recognizing the tyrosine phosphorylated form of MT1-MMP (20), we observed that



overexpression of the wild-type form of MT1-MMP was correlated with increased phosphorylation of the enzyme, particularly when cells were grown within (3D) type I collagen gels (Figure 1A). By contrast, the tyrosine phosphorylation of MT1-MMP was reduced in cells expressing the non-phosphorylatable version of the enzyme, indicating that the mutant acts in a dominant-negative manner in these cells [Figure 1A, (20)]. Due to elevated turnover of the enzyme (23,24), MT1-MMP was expressed at relatively low levels at the surface of both control and stably transfected cells grown atop (2D) collagen (Figure 1B); however, this cell surface localization was significantly increased in cells overexpressing the wild-type as well as the non-phosphorylatable forms of MT1-MMP in cells grown within (3D) type I collagen gels (Figure 1B). Moreover, although MT1-MMP messenger RNA levels were similar in cells overexpressing either the wild-type or the non-phosphorylatable forms of the enzyme (Figure 1C), MT1-MMP was expressed in a higher extent in cells expressing the non-phosphorylatable form (Y573F) of the enzyme (Figure 1A and B), possibly due to reduced internalization caused by the lack of LLY⁵⁷³ cytoplasmic motif (15). Interestingly, confocal images of HT-1080 cells embedded in collagen gels showed that overexpression of wild-type MT1-MMP increased tyrosine phosphorylation of the enzyme and spreading of the cells within the collagen gel, whereas cells expressing the non-phosphorylatable MT1-MMP mutant had markedly reduced levels of phosphorylated MT1-MMP and showed a compact, spherical configuration (Figure 1D).

We next examined the impact of tyrosine phosphorylation on MT1-MMP-mediated tumor cell proliferation. Cells expressing either the empty vector (pcDNA), the wild-type form of MT1-MMP or the non-phosphorylatable version of the enzyme showed similar proliferation rates on 2D collagen, with an exponential growth phase occurring between day 3 and 5 (Figure 2A). By contrast, when cells were embedded within a 3D collagen matrix, basal (pcDNA) tumor cell proliferation was significantly reduced, as previously reported (13), but could be significantly increased by overexpression of wild-type MT1-MMP (2.4-fold compared with control cells at day 7). Interestingly, however, although all transfected cells were viable (Figure 2B), those expressing the non-phosphorylatable form of MT1-MMP showed markedly reduced proliferative rates in the 3D collagen gel, with 50 and 80% inhibition of cell proliferation compared with pcDNA- and wild-type MT1-MMP-transfected cells, respectively (Figure 2A). Similar results were observed when cells were grown within a 3D fibrin matrix (C.Nyalendo, unpublished observations). The inhibitory effect on cell proliferation by the non-phosphorylatable form of MT1-MMP suggests that impaired tyrosine phosphorylation of MT1-MMP reduces tumor cell proliferation in 3D collagen gels triggered by this enzyme.

We next examined if the inhibition of tumor cell proliferation of cells expressing the non-phosphorylatable MT1-MMP mutant was related to alterations in the proteolytic activity of the enzyme. As expected, the growth of tumor cells within 3D collagen matrix (but not on 2D) was abolished by TIMP-2 (but not TIMP-1) as well as by the synthetic MMP inhibitor GM6001, illustrating the crucial role of collagenolysis in this process [Figure 2C, (13)]. However, we observed that cells expressing either the wild-type MT1-MMP or the Y573F mutant both activate pro-MMP-2 to its active form and had similar collagenolytic activities, as reflected by the quantitation of hydroxyproline released from the collagen matrices (Figure 2D). In fact, since HT-1080 cells expressing the MT1-MMP mutant have

a much lower proliferation rate in 3D collagen matrices (see Figure 2A), the amount of hydroxyproline released per cell was 8-fold higher for these cells than for those expressing wild-type MT1-MMP (Figure 2D), further emphasizing that the inhibitory effect of the MT1-MMP mutant on tumor cell proliferation is not related to defective proteolysis.

These results thus indicate that MT1-MMP-mediated proteolysis is not only necessary to confer tumor cells with a proliferative advantage within a 3D collagen matrix but also raises the intriguing possibility that the catalytic activity of the enzyme may not be sufficient for this process.

Impaired tyrosine phosphorylation of MT1-MMP induces cell cycle alterations in tumor cells embedded within 3D collagen gels

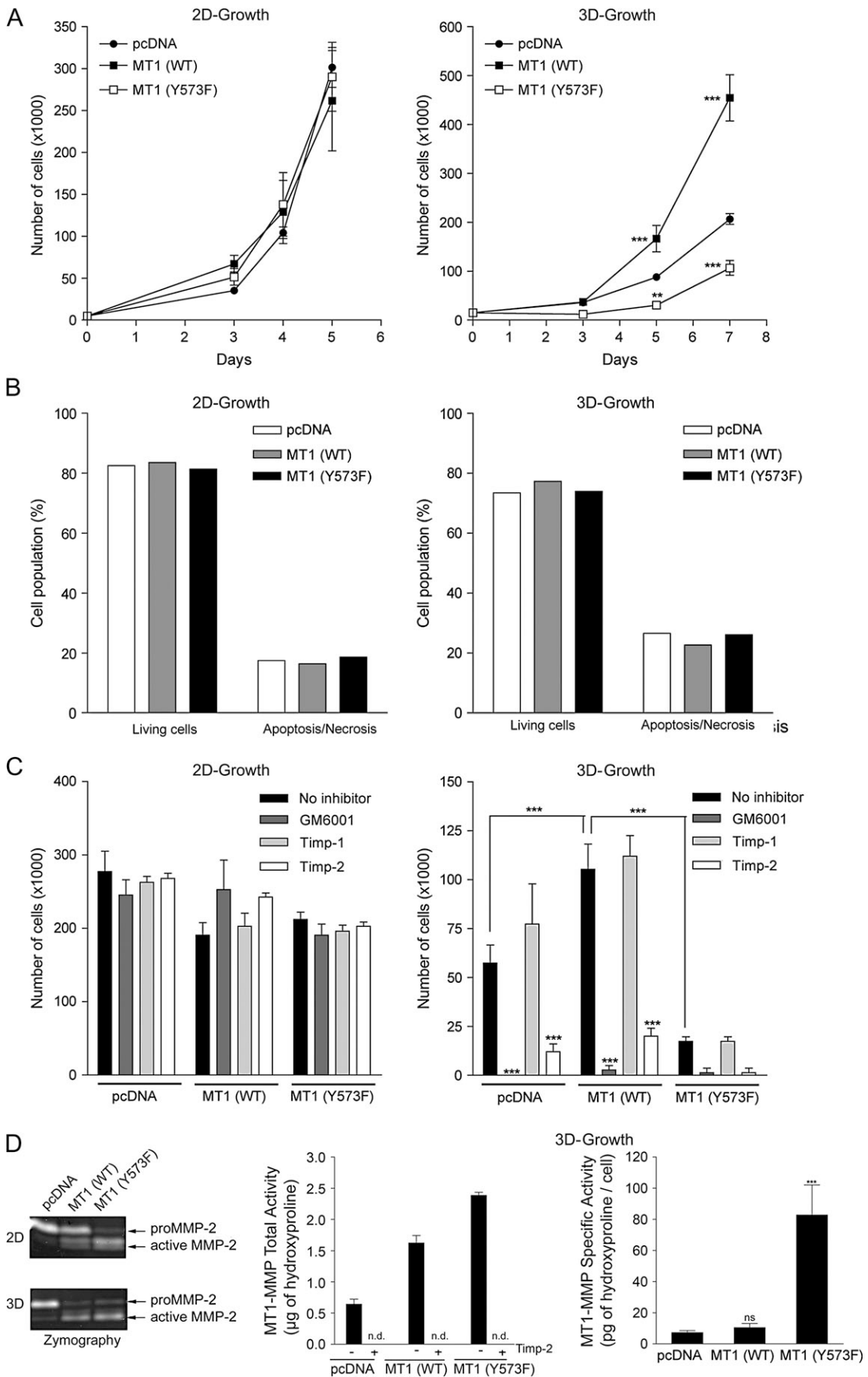
It was previously reported that MT1-MMP-dependent cell proliferation within 3D collagen gels correlated with increased cyclin D₃ kinase activity (13), suggesting a functional coupling between proteolysis of the surrounding collagen matrix and cell cycle progression. As shown in Figure 3A, when grown under planar conditions, cell cycle progression of the HT-1080 transfectants was similar, with almost half of the cells in quiescence (G₀/G₁), and the other half in growth phases (S and G₂/M). Although cells overexpressing the non-phosphorylatable mutant showed proliferation rates similar to those expressing the wild-type version of MT1-MMP (Figure 2A), a small but significant increase of cells in G₀/G₁ as well as a decrease in G₂/M phases were routinely observed. These effects were, however, more pronounced in cells grown within 3D collagen gels, with most of the cells expressing wild-type MT1-MMP in growth phases (S and G₂/M), while expression of the MT1-MMP Y573F mutant markedly increased the proportion of quiescent cells (10% more cells in G₀/G₁), concomitant with a significant diminution of proliferative cells (G₂/M) (Figure 3A). Such an induction of cell growth arrest in 3D by non-phosphorylatable MT1-MMP was correlated with diminution of cyclin D₃ and cyclin-dependent kinase 4 levels (no significant changes were observable for cyclin D₁). Furthermore, the non-phosphorylatable form of MT1-MMP induced a dramatic increase of the cyclin-dependent kinase 4/6 inhibitor p16^{INK4A} (while p15^{INK4B} levels were not modulated), being observable only when cells were grown in 3D collagen matrix (Figure 3B).

Analysis of DNA content by flow cytometry also indicated that overexpression of MT1-MMP leads to aneuploidy, as recently reported (25), with 9.9% of the wild-type MT1-MMP-expressing cells showing an aberrant DNA content (up to 8n), compared with only 5.8% for control cells (Figure 3C). In addition to its inhibitory effect on cell cycle progression, impairment of tyrosine phosphorylation of MT1-MMP completely reversed this MT1-MMP-induced polyploidy in fibrosarcoma cells, with only 5.1% of the non-phosphorylatable MT1-MMP-expressing cells showing aberrant DNA content (Figure 3C). These results thus suggest that the reduction of cell proliferation induced by the non-phosphorylatable MT1-MMP mutant may be related to an inhibitory effect of the mutant on cell cycle progression.

Tyrosine phosphorylation of MT1-MMP is important for invasion of collagen barriers by tumor cells

We next investigated the involvement of tyrosine phosphorylation of MT1-MMP on tumor cell invasion of collagen barriers. When seeded

Fig. 1. Impairment of MT1-MMP tyrosine phosphorylation alters cell morphology of HT-1080 fibrosarcoma cells. HT-1080 cells were stably transfected with wild-type MT1-MMP (MT1 WT), its non-phosphorylatable version (MT1 Y573F) or with the empty vector (pcDNA). For 2D growth, stable transfectants were seeded atop of a collagen film, and for 3D growth, cells were embedded within collagen gels (3D). (A) Total cellular content of MT1-MMP and phospho-MT1-MMP was assessed by western blot; IP: immunoprecipitation, ID: immunodetection, H: immunoglobulin heavy chain. (B) MT1-MMP cell surface expression was monitored by flow cytometry. Black areas represent the control isotype (IgG), gray lines represent MT1-MMP. (C) Stable transfectants were grown in 3D collagen matrix during 5 days. Cells were harvested for messenger RNA (mRNA) isolation and equal amounts were used to prepare cDNA, which was used to assess MT1-MMP gene expression by quantitative polymerase chain reaction. MT1-MMP messenger RNA expression was normalized with β -actin expression as internal control. (D) Stable transfectants were grown in 3D collagen matrix during 5 days and confocal images were obtained from paraffin-embedded sections, as described in Materials and Methods. The white scale bar represents 50 μ m.



atop type I collagen gel, the endogenous MT1-MMP levels of HT-1080 cells confers these cells with the ability to invade the collagen gels to a significant extent; however, overexpression of wild-type MT1-MMP promoted a marked increase in these invasive properties and, as expected, this invasion program required the catalytic activity of the enzyme, as reflected by its sensitivity to TIMP-2 and GM6001 (Figure 4A). By contrast, the invasive potential of cells expressing the non-phosphorylatable MT1-MMP mutant was dramatically decreased, being 8-fold lower than cells expressing its wild-type counterpart and 3-fold lower than control HT-1080 cells. Similar results were also observed when cells were allowed to invade a more dense (2.2 mg/ml) collagen gel; histological analysis of cross-sections from these gels showed that invasion of the gel was significantly increased by expression of wild-type MT1-MMP, whereas cells expressing the non-phosphorylatable MT1-MMP mutant mostly remained at the surface (red arrows, Figure 4B).

Tyrosine phosphorylation of MT1-MMP is important for anchorage-independent growth of tumor cells

We next monitored the effect of the non-phosphorylatable MT1-MMP on the anchorage-independent growth of HT-1080 cells. As shown in Figure 5, control HT-1080 cells formed a significant number of colonies in soft agar but overexpression of wild-type MT1-MMP had no effect on the total number of colonies, as reported (26), although it significantly increased the size and the number of large (macroscopic) colonies. Interestingly, expression of the non-phosphorylatable MT1-MMP mutant antagonized these anchorage-independent growth properties of fibrosarcoma cells, with a 3-fold reduction in the number of colonies formed in soft agar. Since the growth of HT-1080 cells in soft agar does not require the proteolytic activity of MT1-MMP (26), these results provide additional support for an important role of the phosphorylated form of the enzyme in cell proliferation, independent of the intrinsic catalytic activity of the enzyme.

Tyrosine phosphorylation-defective MT1-MMP abrogates the growth of human fibrosarcoma xenografts

To examine the impact of impaired tyrosine phosphorylation of MT1-MMP on tumor growth *in vivo*, stably transfected HT-1080 clones expressing wild-type MT1-MMP, the non-phosphorylatable version of the enzyme or the empty vector, were implanted in mice and tumor size was monitored 34 days postimplantation. As shown in Figure 6A, both pcDNA (5/8) and wild-type MT1-MMP-expressing (7/7) fibrosarcoma cells induced the formation of tumors in nude mice and overexpression of MT1-MMP inducing a significant increase in the mean tumor size. Interestingly, fibrosarcoma cells expressing the non-phosphorylatable version of MT1-MMP failed to grow and form tumors (1/6 for clone a and 0/6 for clone b), even 3 months postimplantation (C. Nyalendo, unpublished observations).

Histological analysis of xenografts formed by the wild-type MT1-MMP-expressing cells revealed a poorly differentiated malignant tumor formed by a majority of spindle cells associated with round cells. The presence of nuclear atypical (black arrows) as well as mitotic figures (yellow arrows) indicates highly active cellular proliferation and characteristic of tumor cells (Figure 6B, HPS), whereas CD31 immunostaining of endothelial cells shows an elevated number of tumor-associated blood vessels (Figure 6B). MT1-MMP was expressed by the majority of the tumor cells but, interestingly, the distribution of the phosphorylated form of the enzyme appears to be

much more restricted, being predominantly detected in cells located at the proximity of blood vessels (Figure 6B).

Although the absence of tumor growth in animals implanted with cells expressing the non-phosphorylatable MT1-MMP mutant precludes a detailed analysis of these tumor cells *in vivo*, preliminary experiments revealed that fibrosarcoma cells expressing either the wild-type or the mutated version of MT1-MMP induced the development of small lesions (microtumors) with similar volumes ($\sim 40 \text{ mm}^3$) 6 days after subcutaneous implantation. Low magnification histological examination of paraffin sections from these early microtumors showed that these two types of xenografts formed a well-delimited lesion (Figure 6C, HPS, upper panels) and seemed similar at first glance. However, at high magnification, the lesions appeared highly different: the microtumor formed by the wild-type MT1-MMP-expressing cells was mainly formed by tumor cells (Figure 6C, HPS, lower panel), and already contained blood vessels (Figure 6C, CD31 immunostaining); by contrast, the lesions induced by cells expressing the non-phosphorylatable version of MT1-MMP lacked either tumor cells (Figure 6C, HPS, lower panel) or blood vessels (Figure 6C, CD31 immunostaining) and were predominantly composed of mouse immune cells and swollen histiocytes. As expected, MT1-MMP was highly expressed in the microtumor derived from wild-type MT1-MMP-expressing cells, whereas it was absent in that induced by cells expressing the mutant (Figure 6C). Overall, these results indicate that tumor cells expressing the non-phosphorylatable form of MT1-MMP have lost the ability to grow *in vivo*, being rapidly eliminated by the innate immune cells of the animal, further suggesting an important function of tyrosine phosphorylated MT1-MMP in the tumorigenicity of fibrosarcoma cells.

Discussion

Our results confirm previous findings showing that MT1-MMP is indeed a major collagenolytic enzyme that enables tumor cells to cleave 3D barriers of fibrillar collagen and make it permissive for proliferation and migration (12,13,27). Importantly, however, we observed that tumor cells expressing an MT1-MMP point mutant lacking a single tyrosine phosphorylation site within its intracellular domain (Y573) showed markedly impaired invasion and proliferation activities within these 3D type I collagen gels, in spite of similar expression of the enzyme at the cell surface as well as unaltered proteolytic activities toward pro-MMP-2 and fibrillar collagen. These observations thus raise the interesting possibility that the proteolytic activity of MT1-MMP, although essential for the degradation of collagen barriers, may not be sufficient *per se* to sustain the proliferation of tumor cells within a 3D environment and suggest that signals originating from the intracellular domain of the enzyme also participate to this process.

While the importance of the cytoplasmic sequence of MT1-MMP for cell migration and invasion has been repeatedly suggested in recent years (28), the molecular events underlying this requirement still remain largely unknown. Src family kinase-dependent phosphorylation of the unique tyrosine residue located within this sequence was recently suggested as an attractive means by which this regulatory function may be achieved, based on the relocalization of the tyrosine phosphorylated form of MT1-MMP at the leading edge of migrating cells (20,21) as well as by the potent inhibitory effect of a dominant-negative, non-phosphorylatable MT1-MMP mutant on cell locomotion

Fig. 2. Inhibition of tumor cell proliferation in 3D collagen matrices by a non-phosphorylatable MT1-MMP mutant. HT-1080 cells were stably transfected with wild-type MT1-MMP (MT1 WT), its non-phosphorylatable version (MT1 Y573F) or with the empty vector (pcDNA). For 2D growth, stable transfectants were seeded (5×10^5 cells) atop of a collagen film, and for 3D growth, 15×10^3 cells were embedded within collagen gels (3D). (A) Time-dependent cell proliferation of HT-1080 transfectants in 2D and 3D collagen matrices. Cells were allowed to grow on 2D or within 3D collagen matrices during the indicated periods of time. (B) Cells were double stained with Annexin V–PI for viability/apoptosis analysis. (C) MT1-MMP-dependent 3D growth was determined by the use of TIMP-1 (broad MMP inhibitor, except MT1-MMP), TIMP-2 and GM6001 (broadly active MMP inhibitor). Cells were allowed to grow on 2D–3D collagen matrix during 5 days. (D) Determination of MT1-MMP catalytic activity. Conditioned media were analyzed for MT1-MMP-dependent activation of MMP-2 by zymography and hydroxyproline (collagen degradation product) content. n.d., not detected; n.s., not significant. Data are means \pm SDs, ** $P < 0.01$, *** $P < 0.001$.

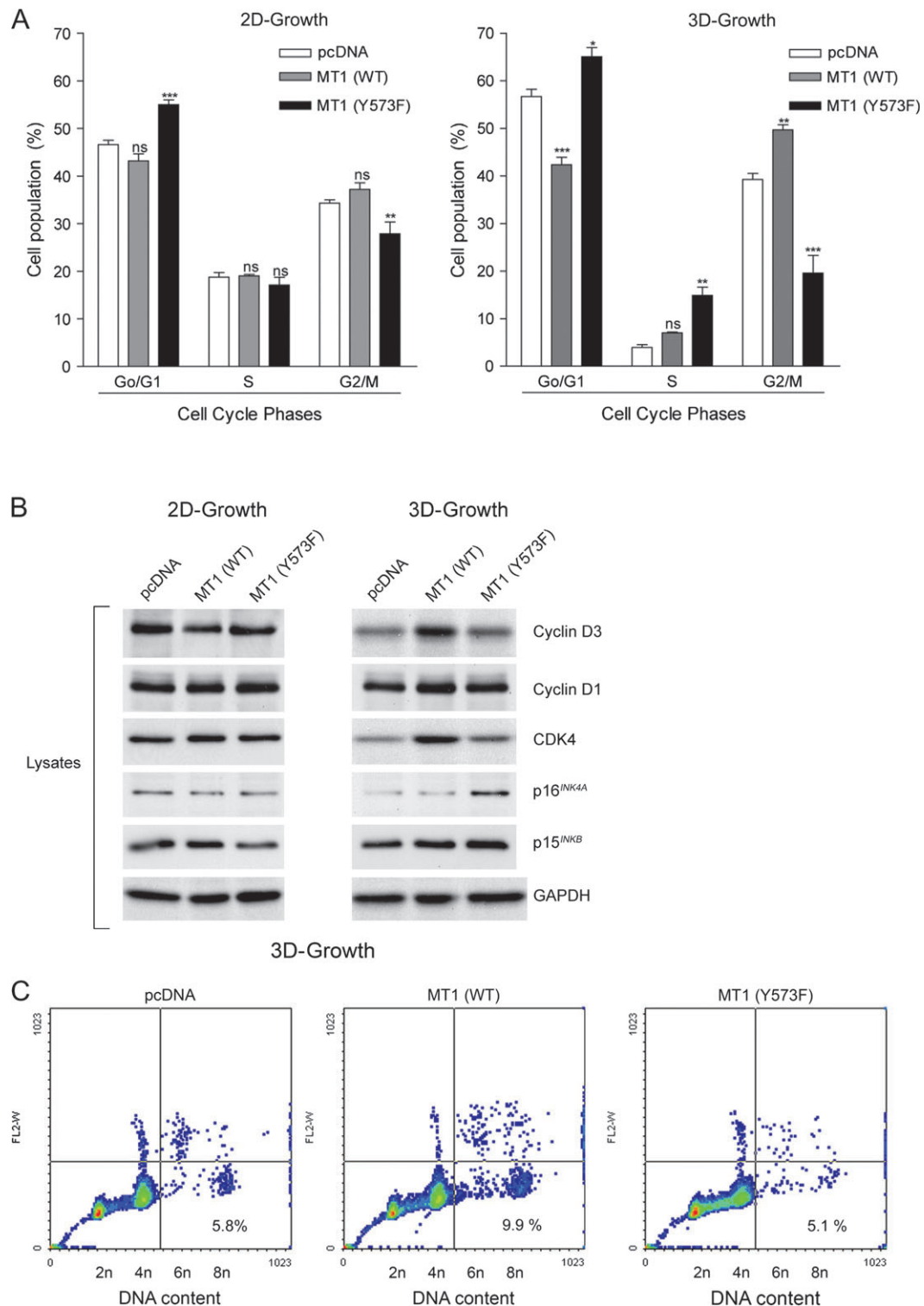


Fig. 3. Cell cycle analysis of HT-1080 cells expressing wild-type MT1-MMP or Y573F mutant in 2D and 3D collagen matrices. HT-1080 cells stably transfected with wild-type MT1-MMP (MT1 WT), its non-phosphorylatable form [MT1 (Y573F)] or with the empty vector (pcDNA) were allowed to grow atop of collagen film (2D) or within collagen gel (3D) during 5 days. Cells were then extracted from 2D and 3D collagen matrices. (A) Cells were analyzed for cell cycle by flow cytometry. (B) Total cellular content of cell cycle markers was assessed by western blot. (C) Aneuploidy was determined by analysis of DNA content. Data are means \pm SDs, * $P < 0.05$; ** $P < 0.01$; *** $P < 0.001$, ns: $P > 0.05$, non-significant.

(20). Results from the current work support such an important role of tyrosine-phosphorylated MT1-MMP by showing that decreased tyrosine phosphorylation of the endogenous enzyme mediated by expression of a non-phosphorylatable MT1-MMP mutant was correlated with

a marked reduction of the invasiveness and proliferation of fibrosarcoma cells embedded in a type I fibrillar collagen network. This inhibitory effect was independent of the enzyme's proteolytic activity but correlated with major alterations in the cell cycle of cells growing

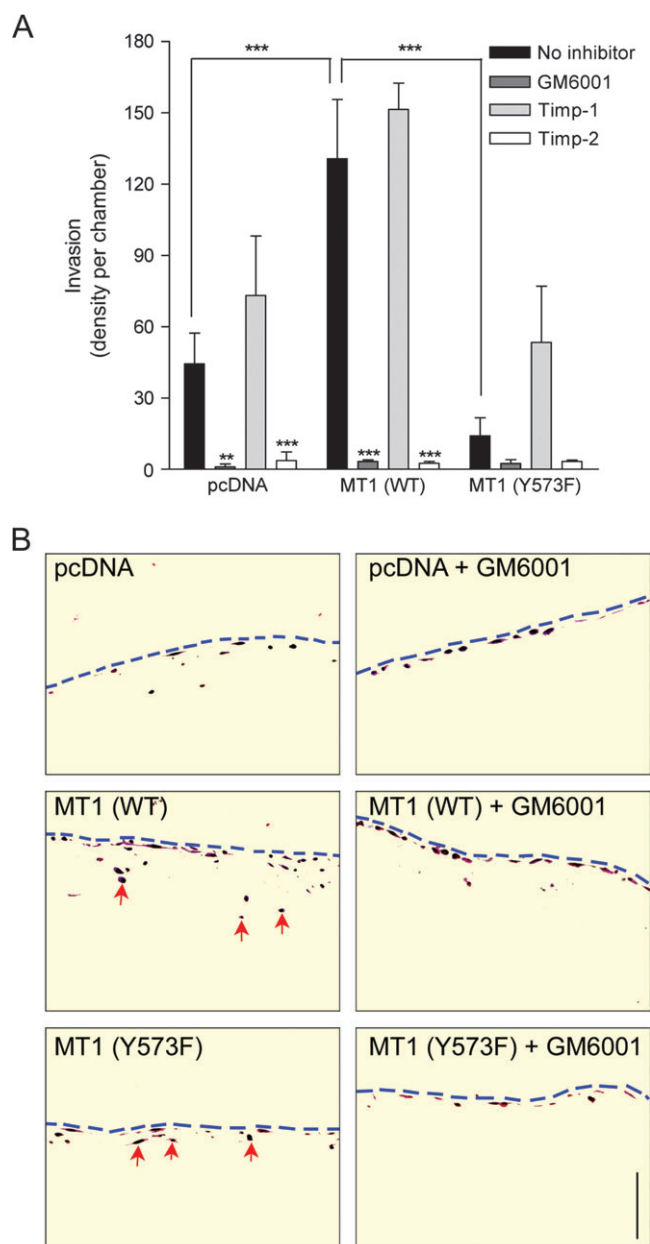


Fig. 4. Inhibition of tumor cell invasion of collagen gels by a non-phosphorylatable MT1-MMP. HT-1080 cells were stably transfected with wild-type MT1-MMP (MT1 WT), its non-phosphorylatable version (MT1 Y573F) or with the empty vector (pcDNA). (A) A total of 5×10^4 cells seeded in Transwells were allowed to invade collagen gel (0.5 mg/ml) during 48 h. (B) A total of 2×10^4 cells were allowed to invade dense collagen gel (2.2 mg/ml) during 8 days. Cross-sections of gels were stained with HPS. Blue dotted lines are the top of the collagen gels. Data are means \pm SDs, $**P < 0.01$; $***P < 0.001$, ns: $P > 0.05$, not significant. Scale bar represents 100 μ m.

in the 3D environment. We observed that the wild-type version of MT1-MMP increases the activity of the cell cycle machinery, leading to enhanced proliferation and to an increase in the aberrant DNA content of HT-1080 cells. However, the expression of the non-phosphorylatable MT1-MMP mutant downregulated cyclin D₃ and cyclin-dependent kinase 4 levels, and increased considerably the levels of the cytostatic mediator p16^{INK4A}, resulting in cell cycle arrest in G₀/G₁ and to the reversal of polyploidy. This suggests that impaired tyrosine phosphorylation of MT1-MMP may counteract the cell cycle

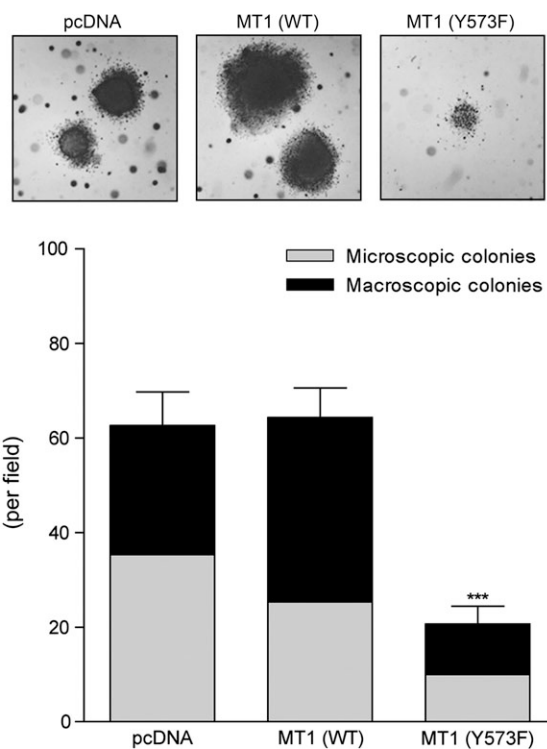


Fig. 5. Inhibition of anchorage-independent growth by a non-phosphorylatable MT1-MMP. HT-1080 cells were stably transfected with wild-type MT1-MMP (MT1 WT), its non-phosphorylatable version (MT1 Y573F) or with the empty vector (pcDNA). Cells were allowed to grow in 0.35% soft agar during 15 days. Macroscopic colonies (visible to the naked eye) and microscopic colonies were counted.

changes normally induced by the enzyme, such as increased cyclin D₃ kinase activity (13).

Although the upstream mechanisms responsible for the inhibitory effect of the non-phosphorylatable MT1-MMP mutant on tumor cell proliferation remain to be more investigated, it is tempting to speculate that the formation of molecular complexes containing tyrosine-phosphorylated MT1-MMP and key signaling intermediates, such as tyrosine-phosphorylated caveolin-1 (20) or p130Cas (21), may participate to the regulation of key cell cycle checkpoints and confer a growth advantage to tumor cells embedded within 3D collagen gels. In this respect, it is noteworthy that at least one of the currently identified proteins that interact with tyrosine-phosphorylated MT1-MMP, p130Cas, acts as a positive regulator of both proliferation and survival in normal and transformed mammary epithelial cells by activating signaling pathways leading to cell cycle progression (29). Such an interference of the MT1-MMP mutant with signaling pathways leading to cell cycle progression would also explain the inhibitory effect of the mutant on anchorage-independent growth of HT-1080 cells in soft agar, a prominent feature of tumorigenic cells that is independent of proteolysis (26) but rather reflects major alterations in cell cycle machinery and in the organization of the cell's cytoskeleton (30). In addition, since aneuploidy is the outcome of deregulation of the cell cycle progression through alteration of the mitotic checkpoint (31) and that MT1-MMP has been shown to confer aneuploidy and tumorigenicity to non-malignant epithelial cells by the MT1-MMP-mediated proteolytic degradation of pericentrin (25), it is possible that the reversal of polyploidy mediated by the MT1-MMP mutant observed in the current study may be related to an inhibitory effect on these processes. Although these mechanisms remain to be identified at the molecular level, these results nevertheless suggest that tyrosine phosphorylation of the intracellular

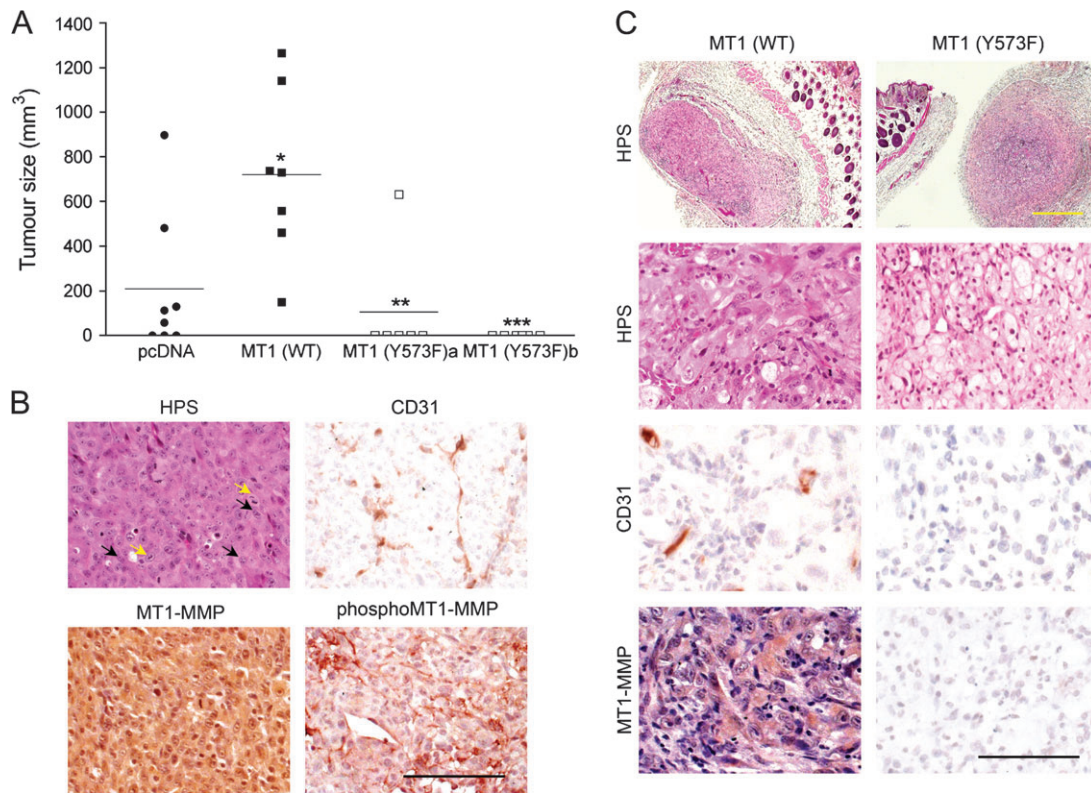


Fig. 6. Inhibition of tumor growth by the non-phosphorylatable MT1-MMP mutant. A total of 5×10^6 HT-1080 cells stably transfected with wild-type MT1-MMP (MT1 WT), its non-phosphorylatable version (MT1 Y573F) or with the empty vector (pcDNA) were implanted subcutaneous in athymic nude mice. (A) Xenografts size after 34 days. $n = 8$ for pcDNA, $n = 7$ for wild-type MT1-MMP (MT1 WT), $n = 6$ for each clone of Y573F MT1-MMP [MT1 (Y573)a and MT1 (Y573)b]. (B) Histological analysis and immunostaining of paraffin-embedded wild-type MT1-MMP-derived xenografts 34 days postimplantation. (C) Histological analysis and immunostaining of paraffin-embedded lesions derived from wild-type MT1-MMP- or the Y573F mutant-expressing fibrosarcoma cells 6 days postimplantation. * $P < 0.05$; ** $P < 0.01$. Black scale bar represents 50 μm ; yellow scale bar represents 1 mm.

domain of MT1-MMP may play an instrumental role in the tumorigenic properties of cancer cells.

In this respect, we observed that an important consequence of the inhibitory effect of the phosphorylation-defective MT1-MMP mutant on tumor cell proliferation and invasion is its ability to prevent tumor growth in nude mice. HT-1080 formed well-defined tumors containing numerous blood vessels and rapidly proliferating cells, as reported previously (32). Although all tumor cells express MT1-MMP, we observed that the tyrosine phosphorylated form of the enzyme was restricted to a subset of tumor cells located at the vicinity of tumor-associated vessels. Since tumor cells at proximity of these blood vessels are exposed to higher oxygen concentrations and divide more rapidly (33,34), the preferential tyrosine phosphorylation of MT1-MMP in these proliferating cells supports a potential important role of the phosphorylated protein in tumor cell proliferation and strengthen the hypothesis that the dominant-negative effect of the MT1-MMP mutant against tyrosine phosphorylation of endogenous MT1-MMP observed *in vitro* is responsible for the antitumor activity of the mutant *in vivo*.

Our results stand in contrast to previous studies showing that in otherwise invasion-incompetent cells, overexpression of a MT1-MMP mutant lacking the entire cytoplasmic sequence confers these cells with the ability to proliferate within collagen gels and to invade ECM barriers similar to that induced by the wild-type enzyme (13,27,35). Although this discrepancy remains to be solved, we posit that the dominant-negative MT1-MMP mutant impairs tyrosine phosphorylation of the endogenous MT1-MMP pool, inducing competition for the activation of the cell autonomous invasion program. This competition would lead to reduced cell cycle progression and proliferation, notwithstanding adequate proteolysis of the surrounding 3D matrix. By

contrast, in cells expressing the cytoplasmic domain-deleted mutant, pericellular proteolysis induced by the enzyme releases the growth constraints induced by the 3D environment, without any interference with the intrinsic cell invasion program, and would thus be sufficient to confer cells within a 3D growth advantage and to sustain tumor progression (13). However, an essential role of the intracellular domain of MT1-MMP for the growth of poorly invasive MCF-7 cells *in vivo* was recently reported (19), suggesting that a requirement for this domain may also depend on the intrinsic invasion program of the recipient cells.

During tumor progression, cancer cells must traverse and grow within an extremely dense 3D barrier composed of ECM proteins (36,37). Recently, MT1-MMP-mediated pericellular proteolysis of the ECM has emerged as an essential mechanism by which tumor cells circumvent the mechanical coercion imposed by these 3D barriers and acquire the ability to invade and proliferate within this growth-restrictive environment (13). The results presented in the current paper suggest that this proteolytic event must also be tightly coupled to intracellular-signaling events in order to sustain proliferation of tumor cells in 3D matrices of which tyrosine phosphorylation of MT1-MMP may play a prominent role. Identification of proteins that specifically interact with tyrosine-phosphorylated MT1-MMP, which is currently underway, should provide important information on the intracellular-signaling pathways responsible for the coupling of MT1-MMP-mediated pericellular proteolysis to tumor cell proliferation.

Funding

Canadian Institutes for Health Research to R.B. and D.G. (MOP62918).

Acknowledgements

We thank Marie-Paule Lachambre for helpful advice on flow cytometry and real-time quantitative polymerase chain reaction.

Conflict of Interest Statement: None declared.

References

- Egeblad, M. *et al.* (2002) New functions for the matrix metalloproteinases in cancer progression. *Nat. Rev. Cancer*, **2**, 161–174.
- Edwards, D.R. *et al.* (1998) Cancer. Proteases—invaders and more. *Nature*, **394**, 527–528.
- Folgueras, A.R. *et al.* (2004) Matrix metalloproteinases in cancer: from new functions to improved inhibition strategies. *Int. J. Dev. Biol.*, **48**, 411–424.
- van Hinsbergh, V.W. *et al.* (2006) Pericellular proteases in angiogenesis and vasculogenesis. *Arterioscler. Thromb. Vasc. Biol.*, **26**, 716–728.
- Pei, D. *et al.* (1996) Transmembrane-deletion mutants of the membrane-type matrix metalloproteinase-1 process progelatinase A and express intrinsic matrix-degrading activity. *J. Biol. Chem.*, **271**, 9135–9140.
- d'Ortho, M.P. *et al.* (1997) Membrane-type matrix metalloproteinases 1 and 2 exhibit broad-spectrum proteolytic capacities comparable to many matrix metalloproteinases. *Eur. J. Biochem.*, **250**, 751–757.
- Hiraoka, N. *et al.* (1998) Matrix metalloproteinases regulate neovascularization by acting as pericellular fibrinolysins. *Cell*, **95**, 365–377.
- Kajita, M. *et al.* (2001) Membrane-type 1 matrix metalloproteinase cleaves CD44 and promotes cell migration. *J. Cell Biol.*, **153**, 893–904.
- Belkin, A.M. *et al.* (2001) Matrix-dependent proteolysis of surface transglutaminase by membrane-type metalloproteinase regulates cancer cell adhesion and locomotion. *J. Biol. Chem.*, **276**, 18415–18422.
- Nakada, M. *et al.* (1999) Expression and tissue localization of membrane-type 1, 2, and 3 matrix metalloproteinases in human astrocytic tumors. *Am. J. Pathol.*, **154**, 417–428.
- Zhai, Y. *et al.* (2005) Expression of membrane type 1 matrix metalloproteinase is associated with cervical carcinoma progression and invasion. *Cancer Res.*, **65**, 6543–6550.
- Sabeh, F. *et al.* (2004) Tumor cell traffic through the extracellular matrix is controlled by the membrane-anchored collagenase MT1-MMP. *J. Cell Biol.*, **167**, 769–781.
- Hotary, K.B. *et al.* (2003) Membrane type I matrix metalloproteinase usurps tumor growth control imposed by the three-dimensional extracellular matrix. *Cell*, **114**, 33–45.
- Lehti, K. *et al.* (2000) Regulation of membrane-type-1 matrix metalloproteinase activity by its cytoplasmic domain. *J. Biol. Chem.*, **275**, 15006–15013.
- Uekita, T. *et al.* (2001) Cytoplasmic tail-dependent internalization of membrane-type 1 matrix metalloproteinase is important for its invasion-promoting activity. *J. Cell Biol.*, **155**, 1345–1356.
- Langlois, S. *et al.* (2004) Membrane type 1-matrix metalloproteinase (MT1-MMP) cooperates with sphingosine 1-phosphate to induce endothelial cell migration and morphogenic differentiation. *Blood*, **103**, 3020–3028.
- Gingras, D. *et al.* (2001) Activation of the extracellular signal-regulated protein kinase (ERK) cascade by membrane-type-1 matrix metalloproteinase (MT1-MMP). *FEBS Lett.*, **507**, 231–236.
- Labrecque, L. *et al.* (2004) Src-mediated tyrosine phosphorylation of caveolin-1 induces its association with membrane type 1 matrix metalloproteinase. *J. Biol. Chem.*, **279**, 52132–52140.
- D'Alessio, S. *et al.* (2008) Tissue inhibitor of metalloproteinases-2 binding to membrane-type 1 matrix metalloproteinase induces MAPK activation and cell growth by a non-proteolytic mechanism. *J. Biol. Chem.*, **283**, 87–99.
- Nyalendo, C. *et al.* (2007) Src-dependent phosphorylation of membrane type I matrix metalloproteinase on cytoplasmic tyrosine 573: role in endothelial and tumor cell migration. *J. Biol. Chem.*, **282**, 15690–15699.
- Gingras, D. *et al.* (2008) Sphingosine-1-phosphate induces the association of membrane-type 1 matrix metalloproteinase with p130Cas in endothelial cells. *FEBS Lett.*, **582**, 399–404.
- Creemers, L.B. *et al.* (1997) Microassay for the assessment of low levels of hydroxyproline. *Biotechniques*, **22**, 656–658.
- Lehti, K. *et al.* (2002) Oligomerization through hemopexin and cytoplasmic domains regulates the activity and turnover of membrane-type 1 matrix metalloproteinase. *J. Biol. Chem.*, **277**, 8440–8448.
- Lehti, K. *et al.* (1998) Proteolytic processing of membrane-type-1 matrix metalloproteinase is associated with gelatinase A activation at the cell surface. *Biochem. J.*, **334** (Pt 2), 345–353.
- Golubkov, V.S. *et al.* (2006) Membrane type-1 matrix metalloproteinase confers aneuploidy and tumorigenicity on mammary epithelial cells. *Cancer Res.*, **66**, 10460–10465.
- Li, Y. *et al.* (2004) Cleavage of lumican by membrane-type matrix metalloproteinase-1 abrogates this proteoglycan-mediated suppression of tumor cell colony formation in soft agar. *Cancer Res.*, **64**, 7058–7064.
- Hotary, K. *et al.* (2000) Regulation of cell invasion and morphogenesis in a three-dimensional type I collagen matrix by membrane-type matrix metalloproteinases 1, 2, and 3. *J. Cell Biol.*, **149**, 1309–1323.
- Itoh, Y. *et al.* (2006) MT1-MMP: a potent modifier of pericellular microenvironment. *J. Cell. Physiol.*, **206**, 1–8.
- Cabodi, S. *et al.* (2006) p130Cas as a new regulator of mammary epithelial cell proliferation, survival, and HER2-neu oncogene-dependent breast tumorigenesis. *Cancer Res.*, **66**, 4672–4680.
- Pawlak, G. *et al.* (2001) Cytoskeletal changes in cell transformation and tumorigenesis. *Curr. Opin. Genet. Dev.*, **11**, 41–47.
- Kops, G.J. *et al.* (2005) On the road to cancer: aneuploidy and the mitotic checkpoint. *Nat. Rev. Cancer*, **5**, 773–785.
- Nonaka, T. *et al.* (2005) Competitive disruption of the tumor-promoting function of membrane type 1 matrix metalloproteinase/matrix metalloproteinase-14 *in vivo*. *Mol. Cancer Ther.*, **4**, 1157–1166.
- Hoogsteen, I.J. *et al.* (2005) Colocalization of carbonic anhydrase 9 expression and cell proliferation in human head and neck squamous cell carcinoma. *Clin. Cancer Res.*, **11**, 97–106.
- Pavelic, Z.P. *et al.* (1981) The relationship of blood vessel proximity and time after radiolabeled thymidine administration to tumor cell population kinetics in a transplanted mouse mammary tumor. *Am. J. Pathol.*, **102**, 84–89.
- Hotary, K. *et al.* (2006) A cancer cell metalloprotease triad regulates the basement membrane transmigration program. *Genes Dev.*, **20**, 2673–2686.
- Even-Ram, S. *et al.* (2005) Cell migration in 3D matrix. *Curr. Opin. Cell Biol.*, **17**, 524–532.
- Hanahan, D. *et al.* (2000) The hallmarks of cancer. *Cell*, **100**, 57–70.

Received March 24, 2008; revised June 27, 2008; accepted July 2, 2008